



Published in final edited form as:

Nature. ; 484(7393): 201–207. doi:10.1038/nature10926.

Teneurins Instruct Synaptic Partner Matching in an Olfactory Map

Weizhe Hong, Timothy J. Mosca, and Liqun Luo

Department of Biology, Howard Hughes Medical Institute Stanford University, Stanford, CA 94305

Abstract

Neurons are interconnected with extraordinary precision to assemble a functional nervous system. Compared to axon guidance, far less is understood about how individual pre- and post-synaptic partners are matched. To ensure the proper relay of olfactory information in flies, axons of ~50 classes of olfactory receptor neurons (ORNs) form one-to-one connections with dendrites of ~50 classes of projection neurons (PNs). Using genetic screens, we identified two evolutionarily conserved EGF-repeat transmembrane Teneurins, Ten-m and Ten-a, as synaptic partner matching molecules between PN dendrites and ORN axons. Ten-m and Ten-a are highly expressed in select PN-ORN matching pairs. Teneurin loss- and gain-of-function cause specific mismatching of select ORNs and PNs. Finally, Teneurins promote homophilic interactions *in vitro*, and Ten-m co-expression in non-partner PNs and ORNs promotes their ectopic connections *in vivo*. We propose that Teneurins instruct matching specificity between synaptic partners through homophilic attraction.

Sperry proposed the chemoaffinity hypothesis nearly 50 years ago to explain the exquisite target specificity of regenerating optic nerves: developing neurons “must carry individual identification tags, presumably cytochemical in nature, by which they are distinguished one from another almost, in many regions, to the level of the single neuron.”¹ Many molecules are now known that guide axons to their target areas^{2,3}, but few may mediate mutual selection and direct matching between individual pre- and post-synaptic partners. Here we show that the transmembrane Teneurins instruct the selection of specific synaptic partners in the *Drosophila* olfactory circuit (Fig. S1).

In *Drosophila*, individual classes of olfactory receptor neuron (ORN) axons make one-to-one connections with individual classes of second-order projection neuron (PN) dendrites within one of ~50 discrete glomeruli in the antennal lobe. We refer to this specific one-to-one connection as PN-ORN synaptic partner matching. Olfactory circuit assembly takes place in sequential steps before sensory activity begins⁴⁻⁶. PN dendrites first elaborate within and pattern the developing antennal lobe⁷⁻⁹, followed by ORN axons invasion¹⁰⁻¹⁴.

Users may view, print, copy, download and text and data- mine the content in such documents, for the purposes of academic research, subject always to the full Conditions of use: http://www.nature.com/authors/editorial_policies/license.html#terms

Correspondence and requests for materials should be addressed to L.L. (lluo@stanford.edu)..

Author Contributions W.H. designed and performed all experiments. T.J.M. assisted in some experiments. L.L. supervised the project. W.H. and L.L. wrote the manuscript with feedback from T.J.M.

Author Information The authors declare no competing financial interests.

Importantly, re-positioning PN dendrites redirects their partner ORN axons without disrupting the connections¹⁵, suggesting that proper PN-ORN connections likely involve direct recognition and matching between partners.

Matching screens identified two Teneurins

To identify potential PN-ORN matching molecules, we simultaneously labeled select PN dendrites and ORN axons in two colors and performed two complementary genetic screens (Fig. 1a,d). We overexpressed 410 candidate cell-surface molecules, comprising ~40% of the potential cell-recognition molecules in *Drosophila*¹⁶. In the first screen, we used *Mz19-GAL4* to label DA1, VA1d and DC3 PNs (hereafter Mz19 PNs), and *Or47b-rCD2* to label Or47b ORNs (Fig. 1a,b). Or47b ORN axons normally project to the VA1m glomerulus and are adjacent to Mz19 PN dendrites without overlap. We overexpressed candidate cell-surface molecules only in Mz19 PNs to identify those that promoted ectopic connections between Or47b axons and Mz19 dendrites (Fig. 1a). We found that overexpression of *ten-m* (*P[GS]9267*, Fig. S2b) produced ectopic connections (Fig. 1c).

In the second screen, we labeled Mz19 PNs as above and Or88a ORNs using *Or88a-rCD2* (Fig. 1d,e). Or88a ORN axons normally project to the VA1d glomerulus, intermingling extensively with VA1d PN dendrites (Fig. 1e). We overexpressed candidate cell-surface molecules in Mz19 PNs (Fig. 1d) as above and found that overexpression of *ten-a* (*P[GE]1914*, Fig. S2a) partially disrupted the intermingling of Or88a axons and Mz19 dendrites (Fig. 1f).

In addition to impairing PN-ORN matching, *ten-m* and *ten-a* overexpression shifted Mz19 PN dendrite position (Fig. 1c,f). However, mismatching was not a secondary consequence of axon or dendrite mispositioning; mispositioning alone, caused by perturbation of other genes, does not alter PN-ORN matching^{9,13,15}. Furthermore, among 410 candidate molecules, only *ten-m* and *ten-a* overexpression exhibited mismatching defects, suggesting their specificity in PN-ORN matching.

Both *ten-m* and *ten-a* appear to encode type II transmembrane proteins¹⁷⁻¹⁹. They possess highly similar domain compositions and amino acid sequences; each contains eight EGF-like and multiple YD (tyrosine-aspartate) repeats within its large C-terminal extracellular domain (Fig. 1g). Ten-m and Ten-a were discovered as Tenascin-like molecules^{20,21}, but vertebrate Teneurins were later identified as their true homologs based on sequence and domain similarity (Fig. 1h). Thus, we refer to Ten-m and Ten-a as *Drosophila* Teneurins. Teneurins are present in nematodes, flies and vertebrates. In human, Teneurin-1 and Teneurin-2 are located in chromosomal regions associated with mental retardation¹⁷, and Teneurin-4 is linked to susceptibility to bipolar disorder²².

Drosophila ten-m was originally identified as a pair-rule gene required for embryonic patterning^{21,23}, but was recently determined otherwise²⁴. Teneurins were implicated in synapse development at the neuromuscular junction^{16,25} (see Ref. 26), and Ten-m also regulates motor axon guidance²⁴. Neither the underlying mechanisms nor their potential roles in the central nervous system are known. Vertebrate Teneurins are widely expressed in

the nervous system^{18,27} and interact homophilically *in vitro*^{28,29}, suggesting their potential role as homophilic cell adhesion molecules in patterning neuronal connectivity.

Matching expression of Teneurins

Both *Drosophila* Teneurins were endogenously expressed in the developing antennal lobe (Fig. 2a, S3). At 48 hrs after puparium formation (APF), when individual glomeruli just become identifiable, elevated Teneurin expression was evident in select glomeruli. The subset of glomeruli expressing elevated Ten-m was distinct but partially overlapping with that expressing elevated Ten-a (Fig. 2a,e). Teneurins were also detected at a low level in all glomeruli. Both basal and elevated Teneurin expressions were eliminated by pan-neuronal RNAi targeting the corresponding gene (Fig. 2b,c), suggesting that Teneurins are produced predominantly by neurons. In a *ten-a* null mutant we generated (Fig. S2a), all Ten-a expression was eliminated, confirming antibody specificity (Fig. 2d).

The antennal lobe consists of ORN axons as well as PN and local interneuron dendrites. We used intersectional analysis to determine the cellular source for elevated Teneurin expression. For *ten-m*, we screened GAL4 enhancer traps near the *ten-m* gene, and identified NP6658 (hereafter as *ten-m-GAL4*; Fig. S2b) that recapitulated the glomerulus-specific Ten-m staining pattern (Fig. S4a-c). We used a FLPout reporter *UAS>stop>mCD8GFP* to determine the intersection of *ten-m-GAL4* and an ORN-specific *ey-Flp* (Fig. 2f, S4d-f) or a PN-specific *GHI46-Flp* (Fig. 2g, S4g-i). We found that *ten-m-GAL4* was selectively expressed in a subset of ORNs and PNs. Due to reagent availability, we focused our analysis on five glomeruli (DA1, VA1d, VA1m, DC3, DA3), adjacently located on the lateral and anterior side of the antennal lobe. In these five glomeruli, Ten-m expression in PN and ORN classes matched: high levels in PNs corresponded to high levels in ORNs and vice versa (Fig. 2f-g).

To determine the cellular origin of elevated Ten-a expression, we performed tissue-specific RNAi of endogenous Ten-a, as no GAL4 enhancer trap is available near *ten-a*. To isolate Ten-a expression in ORNs, we drove pan-neuronal *ten-a* RNAi while specifically suppressing RNAi in ORNs using *tubP>stop>GAL80* and *ey-Flp* (Fig. 2h). To restrict Ten-a expression to central neurons, we expressed *ten-a* RNAi in all ORNs (Fig. 2i). We found that Ten-a was highly expressed in a subset of ORNs and central neurons, and also showed a matching expression in five glomeruli focused here (Fig. 2h-i). The glomerular-specific differential Ten-a expression in central neurons likely arises mainly from PNs as they target dendrites to specific glomeruli, and punctate Ten-a staining was observed in PN cell bodies (Fig. S5). In summary, Ten-m and Ten-a are each highly expressed in a distinct, but partially overlapping, subset of matching ORNs and PNs (Fig. 2j).

Teneurins are required for PN-ORN matching

To examine whether Teneurins are required for proper PN-ORN matching, we performed tissue-specific RNAi (Fig. 3, S2c) in all neurons using *C155-GAL4*, in PNs using *GHI46-GAL4*, or in ORNs using *peb-GAL4*. To label specific subsets of PN dendrites independent of GAL4-UAS, we used the Q binary expression system³⁰, and converted *Mz19-GAL4* to *Mz19-QF* by BAC recombineering (Fig. S2d). We could thus perform GAL4-based RNAi

knockdown while labeling PN dendrites and ORN axons in two colors independent of GAL4. We focused our analysis on Mz19 dendrites and Or47b axons, which innervate neighboring glomeruli but never intermingle in wild type (Fig. 1b, 3a-b).

Pan-neuronal RNAi of both *teneurins* shifted Or47b axons to a position between two adjacent Mz19 glomeruli, DA1 and VA1d (Fig. 3c). Moreover, Mz19 dendrites and Or47b axons intermingled without a clear border (Fig. 3c, d), reflecting a PN-ORN matching defect. We confirmed this using independent RNAi lines targeting different regions of the *ten-m* and *ten-a* transcripts (Fig. S6). Further, knocking down *teneurins* only in PNs or ORNs also led to Mz19-Or47b intermingling (Fig. 3e, S7a,d), indicating that Teneurins are required in both PNs and ORNs to ensure proper matching.

Next, we examined the contribution of each Teneurin by individual RNAi knockdown in ORNs. Knocking down *ten-m*, and to a lesser extent, *ten-a*, caused mild mismatching (Fig. 3e, S7). This was greatly enhanced by simultaneous *teneurin* knockdown (Fig. 3e), likely because Mz19-Or47b mismatching requires weakening connections with their respective endogenous partners (Fig. S7g). This synergy implies that multiple matching molecules can enhance partner matching robustness.

We also tested the functions of individual Teneurins in PNs. We found that the Mz19-Or47b mismatching was caused by PN-specific knockdown of *ten-a*, but not *ten-m* (Fig. 3e, S7). As VA1d/DC3 and DA1 PNs arise from separate neuroblast lineages³¹, we generated MARCM neuroblast clones to label and knock down *ten-a* in DA1 or VA1d/DC3 PNs (Fig. 3f-j, see Methods). *ten-a* knockdown only in DA1 PNs (normally Ten-a high) caused dendrite mismatching with Or47b axons (Fig. 3h-j). By contrast, *ten-a* knockdown in VA1d/DC3 PNs (normally Ten-a low) did not cause mismatching (Fig. 3j, S8a,b). Similarly, MARCM loss-of-function of *ten-a* mutant in DA1 but not in VA1d/DC3 PNs resulted in mismatching with Or47b ORNs (Fig. 3j, S8c-d). Thus, removal of *ten-a* from Ten-a-high DA1 PNs caused dendrite mismatching with Ten-a-low Or47b ORNs (Fig. 3i). The differential requirements of Ten-m and Ten-a in ORNs or PNs in preventing Mz19-Or47b mismatching likely reflect differential expression of Ten-m and Ten-a in the mismatching partners.

Our finding that loss of *ten-a* caused Ten-a-high PNs to mismatch with Ten-a-low ORNs (Fig. 3i,j), together with the matching expression of Teneurins in PNs and ORNs, raised the possibility that Teneurins instruct class-specific PN-ORN connections through homophilic attraction: PNs expressing high-level Ten-m or Ten-a connect to ORNs with high-level Ten-m or Ten-a, respectively.

Teneurins instruct matching specificity

This homophilic attraction hypothesis predicts that overexpression of a given Teneurin in PNs (1) should preferentially affect PNs normally expressing low levels of that Teneurin, causing their dendrites to lose endogenous connections with their cognate ORNs, and (2) should cause these PNs to make ectopic connections with ORNs expressing high levels of that Teneurin.

To test the first prediction, we examined whether Teneurin overexpression in Mz19 PNs impaired their endogenous connections with cognate ORNs. Consistently, Ten-m overexpression specifically disrupted the connections of DA1 PNs and Or67d ORNs, a PN-ORN pair expressing low-level Ten-m (Fig. S9b,e). Connections of the other two pairs were unaffected (Fig. S9a,c,d,f). Likewise, Ten-a overexpression specifically disrupted connections between VA1d PNs and Or88a ORNs, a PN-ORN pair expressing low-level Ten-a (Fig. S9g), but not between the other two PN-ORN pairs (Fig. S9h-i).

To test the second prediction, we examined the specificity of ectopic connections made by Mz19 PNs overexpressing Teneurins, and sampled with non-partner ORN classes that project axons nearby Mz19 dendrites (Fig. S10). We found that Ten-m overexpression in Mz19 PNs caused dendrite mismatching only with Or47b ORNs (Fig. S10f). To examine additional mismatching phenotypes that may occur within Mz19 glomeruli and to determine whether DA1 or VA1d/DC3 PNs contribute to the ectopic connections, we used MARCM to overexpress Ten-m in individual PN classes. We found that Ten-m overexpression in DA1 PNs (Ten-m low) caused dendrite mismatching with Or47b (Fig. 4a-b) and (to a lesser extent) Or88a ORNs (Fig. 4b-c), both endogenously expressing high-level Ten-m. By contrast, Ten-m overexpression in VA1d/DC3 PNs did not produce ectopic connections with any non-matching ORNs tested (Fig. 4d-f).

Likewise, Ten-a overexpression in Mz19 PNs caused dendrite mismatching only with Or23a ORNs among all non-matching ORN classes sampled outside the Mz19 region (Fig. S10l). Further, MARCM overexpression of Ten-a in VA1d/DC3 PNs (Ten-a low) caused dendrite mismatching specifically with Or23a (Fig. 4j-k) and (to a lesser extent) Or67d ORNs (Fig. 4k-l), both endogenously expressing high-level Ten-a (Fig. 4l). By contrast, Ten-a overexpression in DA1 PNs (Ten-a high) did not produce ectopic connections with any non-matching ORNs tested (Fig. 4g-i). Thus, both Ten-m and Ten-a overexpression analyses support the homophilic attraction hypothesis.

Our data also suggest that additional molecule(s) are required to completely determine the wiring specificity of the five PN-ORN pairs examined. For example, VA1d-Or88a and VA11m-Or47b have indistinguishable Ten-m/Ten-a expression patterns (Fig. 2j), and may require additional molecules to distinguish target choice. Indeed, Ten-a knockdown (Fig. 3h-j, S8e-f) or Ten-m overexpression (Fig. 4b,c) caused DA1 PNs to mismatch preferentially with Or47b as opposed to Or88a axons. This suggests that the non-adjacent DA1 and VA11m share a more similar Teneurin-independent cell-surface code than the adjacent VA1d and VA11m. Likewise, Ten-a overexpression caused VA1d PNs to mismatch with the non-adjacent Or23a more so than the adjacent Or67d ORNs, even though both ORNs express high-level Ten-a (Fig. 4k,l). Finally, Ten-m overexpression in DC3 PNs, which express low-level Ten-m, did not change its matching specificity (Fig. 4f, S9f), suggesting that Teneurin-independent mechanisms are involved in matching DC3 PNs and Or83c ORNs.

In summary, we showed that Teneurin overexpression in Teneurin-low PNs caused their dendrites to lose endogenous connections with Teneurin-low ORNs and mismatch with Teneurin-high ORNs (Fig. 4b,k). However, Teneurin overexpression in Teneurin-high PNs

did not disrupt their proper connections (Fig. 4e,h). These data strongly support that Teneurins instruct connection specificity likely through homophilic attraction, by matching Ten-m or Ten-a levels in PN and ORN partners.

Ten-m promotes PN-ORN homophilic attractions

To test whether Teneurins interact *in vitro*, we separately transfected two populations of *Drosophila* S2 cells with FLAG- and HA-tagged Teneurins, and performed co-immunoprecipitations from lysates of these cells after mixing. We detected strong homophilic interactions between FLAG- and HA-tagged Ten-m proteins, and to a lesser extent between FLAG- and HA-tagged Ten-a proteins (Fig. 5a). Ten-m and Ten-a also exhibited heterophilic interactions (Fig. 5a), which may account for their role in synapse organization²⁶.

Next, we tested if Teneurins can homophilically promote *in vivo* trans-cellular interactions between PN dendrites and ORN axons. We simultaneously overexpressed Ten-m in Mz19 PNs using *Mz19-QF*, and Or67a and Or49a ORNs using *AM29-GAL4*³² (Fig. 5b). This enabled us to independently label and manipulate Mz19 dendrites and AM29 axons with distinct markers and transgenes. We chose *AM29-GAL4* because of its early onset of expression, whereas other class-specific ORN drivers start to express only after PN-ORN connection is established^{5,6}. AM29 axons do not normally connect with Mz19 dendrites (Fig. 5c-d).

Simultaneous overexpression of Ten-m in both Mz19 PNs and AM29 ORNs produced ectopic connections between them (Fig. 5c,g), suggesting that Ten-m homophilically promotes PN-ORN attraction. By contrast, Ten-m overexpression only in PNs or ORNs did not produce any ectopic connections, despite causing dendrite or axon mistargeting, respectively (Fig. 5c,e,f). These data ruled out the involvement of heterophilic partners in Ten-m-mediated attraction. Simultaneous overexpression of Ten-a in Mz19 PNs and AM29 ORNs did not produce ectopic connections (not shown), possibly due to lower expression or weaker Ten-a homophilic interactions (Fig. 5a).

Finally, we examined whether these ectopic connections lead to the formation of synaptic structures. Indeed, the ectopic connections between Mz19 dendrites and AM29 axons were enriched in synaptotagmin-HA expressed from AM29 ORNs (Fig. 5h), suggesting that these connections can aggregate synaptic vesicles and could be functional. We propose that Teneurins promote attraction between PN-ORN synaptic partners through homophilic interactions, eventually leading to synaptic connections.

Discussion

Compared to axon guidance, relatively little is known about synaptic target selection mechanisms²⁻⁴. Among the notable examples, the graded expressions of vertebrate EphA and Ephrin-A instruct the topographic targeting of retinal ganglion cell axons^{4,33-35}. Chick DSCAMs and Sidekicks promote lamina-specific arborization of retinal neurons³⁶. *Drosophila* Capricious promotes target specificity of photoreceptor and motor axons^{16,37-39}. *C. elegans* SYG-1 and SYG-2 specify synapse location through interaction between pre-

synaptic axons and intermediate guidepost cells⁴⁰. However, it is unclear whether any of these molecules mediate direct, selective interactions between individual pre- and post-synaptic partners. Indeed, in complex neural circuits, it is not clear *a priori* whether molecular determinants mediate such interactions. For example, the final retinotopic map is thought to result from both Ephrin signaling and spontaneous activity^{41,42}. Mammalian ORN axon targeting involves extensive axon-axon interactions through activity-dependent and independent modes^{43,44}, with minimal participation of postsynaptic neurons identified thus far.

Here, we show that Teneurins instruct PN-ORN matching through homophilic attraction. Although each glomerulus contains many synapses between cognate ORNs and PNs, these synapses transmit the same information and can be considered identical with regard to specificity. Thus, Teneurins represent a strong case in determining connection specificity directly between pre- and post-synaptic neurons. We further demonstrate that molecular determinants can instruct connection specificity of a moderately complex circuit at the level of individual synapses.

Our study reveals a requirement for PN-ORN attraction in the stepwise assembly of the olfactory circuit. PN dendrites and ORN axons first independently target to appropriate regions using global cues, dendrite-dendrite and axon-axon interactions^{8,9,12-14}. These initial, independent dendrite and axon targeting are eventually coordinated in their final one-to-one matching. We identified Teneurins as the first molecules to mediate this matching process, through direct PN-ORN attraction. Our analyses have focused on a subset of ORN-PN pairs involving trichoid ORNs⁴⁵, including Or67d/Or88a/Or47b that are implicated in pheromone sensation⁴⁶. The partially overlapping expressions of Teneurins in other PN and ORN classes (Fig. 2, S4) suggest a broader involvement of Teneurins. At the same time, additional cell-surface molecules are also needed to completely determine connection specificity of all 50 PN-ORN pairs.

Teneurins are present throughout *Animalia* (Fig. 1h). Different vertebrate Teneurins are broadly expressed in distinct and partially overlapping patterns in the nervous system¹⁸. Teneurin-3 is expressed in the visual system and is required for ipsilateral retinogeniculate projections⁴⁷. Our study suggests that differential Teneurin expression may play a general role in matching pre- and post-synaptic partners. Indeed, high-level Ten-m is involved in matching select motoneuron-muscle pairs²⁶. Furthermore, Teneurins also trans-synaptically mediate neuromuscular synapse organization²⁶. This suggests that the synapse partner matching function of Teneurins may have evolved from their basal role in synapse organization. Interestingly, synaptic partner matching only involves homophilic interactions (this study and ref. 26), whereas synapse organization preferentially involves heterophilic interactions²⁶. This could not be fully accounted for by different strength of their homophilic and heterophilic interactions *in vitro* (Fig. 5a). Indeed, while heterophilic interactions occur *in vitro* (Fig. 5a), heterophilic overexpression of Ten-m and Ten-a in AM29 ORNs and Mz19 PNs did not produce ectopic connections (not shown). Thus we speculate that these dual functions of Teneurins *in vivo* may engage signaling mechanisms that further distinguish homophilic versus heterophilic interactions.

METHODS SUMMARY

Detailed methods on fly stocks, generation of the *ten-a* allele, construction of transgenic flies, clonal analysis, histology, imaging, quantification and statistical analysis, epitope-tagged constructs, and co-immunoprecipitation can be found in Methods.

Supplementary Material

Refer to Web version on PubMed Central for supplementary material.

Acknowledgements

We thank V. Favaloro for advice on biochemistry and D. Luginbuhl for technical assistance; K. Zinn for the EP collection; R. Wides and S. Baumgartner for *teneurin* reagents; B. Zhang, Bloomington, Kyoto, and Harvard and Vienna Stock Centers for fly stocks; BestGene Inc. for injection service; and K. Shen, T. Clandinin, D. Berns, V. Favaloro, X. Gao, S. Hippenmeyer, C. Liu, K. Miyamichi, and X. Yu for critiques. Supported by an NIH grant (R01 DC-005982 to L.L.), and Epilepsy, Neonatology and Developmental Biology Training Grants (NIH 5T32 NS007280 and HD007249 to T.J.M.). L.L. is an investigator of the Howard Hughes Medical Institute.

REFERENCES

1. Sperry RW. Chemoaffinity in the orderly growth of nerve fiber patterns and connections. *Proc Natl Acad Sci USA*. 1963; 50:703–710. [PubMed: 14077501]
2. Dickson BJ. Molecular mechanisms of axon guidance. *Science*. 2002; 298:1959–1964. [PubMed: 12471249]
3. Zipursky SL, Sanes JR. Chemoaffinity revisited: dscams, protocadherins, and neural circuit assembly. *Cell*. 2010; 143:343–353. [PubMed: 21029858]
4. Luo L, Flanagan JG. Development of continuous and discrete neural maps. *Neuron*. 2007; 56:284–300. [PubMed: 17964246]
5. Komiyama T, Luo L. Development of wiring specificity in the olfactory system. *Curr Opin Neurobiol*. 2006; 16:67–73. [PubMed: 16377177]
6. Brochtrup A, Hummel T. Olfactory map formation in the *Drosophila* brain: genetic specificity and neuronal variability. *Curr Opin Neurobiol*. 2011; 21:85–92. [PubMed: 21112768]
7. Jefferis GSXE, et al. Developmental origin of wiring specificity in the olfactory system of *Drosophila*. *Development*. 2003; 131:117–130. [PubMed: 14645123]
8. Komiyama T, Sweeney LB, Schuldiner O, Garcia KC, Luo L. Graded expression of semaphorin-1a cell-autonomously directs dendritic targeting of olfactory projection neurons. *Cell*. 2007; 128:399–410. [PubMed: 17254975]
9. Hong W, et al. Leucine-rich repeat transmembrane proteins instruct discrete dendrite targeting in an olfactory map. *Nat. Neurosci*. 2009; 12:1542–1550. [PubMed: 19915565]
10. Hummel T, et al. Axonal targeting of olfactory receptor neurons in *Drosophila* is controlled by Dscam. *Neuron*. 2003; 37:221–231. [PubMed: 12546818]
11. Hummel T, Zipursky SL. Afferent induction of olfactory glomeruli requires N-cadherin. *Neuron*. 2004; 42:77–88. [PubMed: 15066266]
12. Sweeney LB, et al. Temporal target restriction of olfactory receptor neurons by Semaphorin-1a/PlexinA-mediated axon-axon interactions. *Neuron*. 2007; 53:185–200. [PubMed: 17224402]
13. Lattemann M, et al. Semaphorin-1a Controls Receptor Neuron-Specific Axonal Convergence in the Primary Olfactory Center of *Drosophila*. *Neuron*. 2007; 53:169–184. [PubMed: 17224401]
14. Chou Y-H, Zheng X, Beachy PA, Luo L. Patterning axon targeting of olfactory receptor neurons by coupled hedgehog signaling at two distinct steps. *Cell*. 2010; 142:954–966. [PubMed: 20850015]
15. Zhu H, et al. Dendritic patterning by Dscam and synaptic partner matching in the *Drosophila* antennal lobe. *Nat. Neurosci*. 2006; 9:349–355. [PubMed: 16474389]

16. Kurusu M, et al. A Screen of Cell-Surface Molecules Identifies Leucine-Rich Repeat Proteins as Key Mediators of Synaptic Target Selection. *Neuron*. 2008; 59:972–985. [PubMed: 18817735]
17. Tucker RP, Chiquet-Ehrismann R. Teneurins: a conserved family of transmembrane proteins involved in intercellular signaling during development. *Dev Biol*. 2006; 290:237–245. [PubMed: 16406038]
18. Tucker RP, Kenzelmann D, Trzebiatowska A, Chiquet-Ehrismann R. Teneurins: transmembrane proteins with fundamental roles in development. *Int J Biochem Cell Biol*. 2007; 39:292–297. [PubMed: 17095284]
19. Young TR, Leamey CA. Teneurins: important regulators of neural circuitry. *Int J Biochem Cell Biol*. 2009; 41:990–993. [PubMed: 18723111]
20. Baumgartner S, Chiquet-Ehrismann R. Tena, a Drosophila gene related to tenascin, shows selective transcript localization. *Mech. Dev*. 1993; 40:165–176. [PubMed: 7684246]
21. Baumgartner S, Martin D, Hagios C, Chiquet-Ehrismann R. Tenm, a Drosophila gene related to tenascin, is a new pair-rule gene. *EMBO J*. 1994; 13:3728–3740. [PubMed: 8070401]
22. Psychiatric GWAS Consortium Bipolar Disorder Working Group. et al. Large-scale genome-wide association analysis of bipolar disorder identifies a new susceptibility locus near ODZ4. *Nat Genet*. 2011; 43:977–983. [PubMed: 21926972]
23. Levine A, et al. Odd Oz: a novel Drosophila pair rule gene. *Cell*. 1994; 77:587–598. [PubMed: 7514504]
24. Zheng L, et al. Drosophila Ten-m and Filamin Affect Motor Neuron Growth Cone Guidance. *PLoS ONE*. 2011; 6:e22956. [PubMed: 21857973]
25. Liebl FLW, et al. Genome-wide P-element screen for Drosophila synaptogenesis mutants. *J Neurobiol*. 2006; 66:332–347. [PubMed: 16408305]
26. Mosca TJ, Hong W, Dani VS, Favaloro V, Luo L. Transsynaptic Teneurin Signaling in Neuromuscular Synapse Organization and Target Choice. *Nature*. 2012; (this issue)
27. Li H, Bishop KM, O’Leary DDM. Potential target genes of EMX2 include Odz/Ten-M and other gene families with implications for cortical patterning. *Mol. Cell. Neurosci*. 2006; 33:136–149. [PubMed: 16919471]
28. Rubin BP, Tucker RP, Brown-Luedi M, Martin D, Chiquet-Ehrismann R. Teneurin 2 is expressed by the neurons of the thalamofugal visual system in situ and promotes homophilic cell-cell adhesion in vitro. *Development*. 2002; 129:4697–4705. [PubMed: 12361962]
29. Oohashi T, et al. Mouse ten-m/Odz is a new family of dimeric type II transmembrane proteins expressed in many tissues. *J. Cell Biol*. 1999; 145:563–577. [PubMed: 10225957]
30. Potter CJ, Tasic B, Russler EV, Liang L, Luo L. The Q system: a repressible binary system for transgene expression, lineage tracing, and mosaic analysis. *Cell*. 2010; 141:536–548. [PubMed: 20434990]
31. Jefferis GS, Marin EC, Stocker RF, Luo L. Target neuron prespecification in the olfactory map of Drosophila. *Nature*. 2001; 414:204–208. [PubMed: 11719930]
32. Endo K, Aoki T, Yoda Y, Kimura K-I, Hama C. Notch signal organizes the Drosophila olfactory circuitry by diversifying the sensory neuronal lineages. *Nat. Neurosci*. 2007; 10:153–160. [PubMed: 17220884]
33. Drescher U, et al. In vitro guidance of retinal ganglion cell axons by RAGS, a 25 kDa tectal protein related to ligands for Eph receptor tyrosine kinases. *Cell*. 1995; 82:359–370. [PubMed: 7634326]
34. Cheng HJ, Nakamoto M, Bergemann AD, Flanagan JG. Complementary gradients in expression and binding of ELF-1 and Mek4 in development of the topographic retinotectal projection map. *Cell*. 1995; 82:371–381. [PubMed: 7634327]
35. Feldheim DA, et al. Genetic analysis of ephrin-A2 and ephrin-A5 shows their requirement in multiple aspects of retinocollicular mapping. *Neuron*. 2000; 25:563–574. [PubMed: 10774725]
36. Yamagata M, Sanes JR. Dscam and Sidekick proteins direct lamina-specific synaptic connections in vertebrate retina. *Nature*. 2008; 451:465–469. [PubMed: 18216854]
37. Shinza-Kameda M, Takasu E, Sakurai K, Hayashi S, Nose A. Regulation of layer-specific targeting by reciprocal expression of a cell adhesion molecule, capricious. *Neuron*. 2006; 49:205–213. [PubMed: 16423695]

38. Shishido E, Takeichi M, Nose A. Drosophila synapse formation: regulation by transmembrane protein with Leu-rich repeats, CAPRICIOUS. *Science*. 1998; 280:2118–2121. [PubMed: 9641918]
39. de Wit J, Hong W, Luo L, Ghosh A. Role of leucine-rich repeat proteins in the development and function of neural circuits. *Annu Rev Cell Dev Biol*. 2011; 27:697–729. [PubMed: 21740233]
40. Shen K, Fetter RD, Bargmann CI. Synaptic specificity is generated by the synaptic guidepost protein SYG-2 and its receptor, SYG-1. *Cell*. 2004; 116:869–881. [PubMed: 15035988]
41. McLaughlin T, Torborg CL, Feller MB, O’Leary DDM. Retinotopic map refinement requires spontaneous retinal waves during a brief critical period of development. *Neuron*. 2003; 40:1147–1160. [PubMed: 14687549]
42. Pfeiffenberger C, Yamada J, Feldheim DA. Ephrin-As and patterned retinal activity act together in the development of topographic maps in the primary visual system. *J Neurosci*. 2006; 26:12873–12884. [PubMed: 17167078]
43. Imai T, et al. Pre-target axon sorting establishes the neural map topography. *Science*. 2009; 325:585–590. [PubMed: 19589963]
44. Serizawa S, et al. A neuronal identity code for the odorant receptor-specific and activity-dependent axon sorting. *Cell*. 2006; 127:1057–1069. [PubMed: 17129788]
45. Couto A, Alenius M, Dickson BJ. Molecular, anatomical, and functional organization of the Drosophila olfactory system. *Curr Biol*. 2005; 15:1535–1547. [PubMed: 16139208]
46. van der Goes van Naters W, Carlson JR. Receptors and neurons for fly odors in Drosophila. *Curr Biol*. 2007; 17:606–612. [PubMed: 17363256]
47. Leamey CA, et al. Ten_m3 regulates eye-specific patterning in the mammalian visual pathway and is required for binocular vision. *PLoS Biol*. 2007; 5:e241. [PubMed: 17803360]

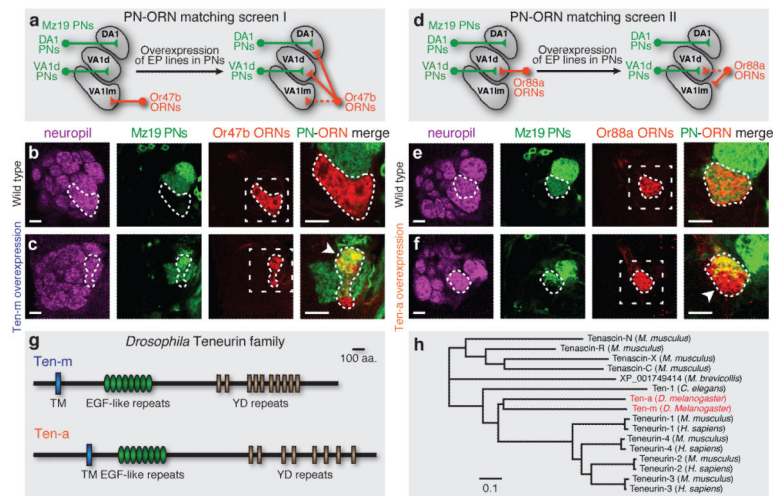


Figure 1. PN-ORN synaptic matching screens identify two Teneurins

a, d, Schematics showing two PN-ORN matching screens. PN dendrites are labeled by *Mz19-GALA* driving mCD8GFP and ORN axons by *Or47b-rCD2* (**a**) or *Or88a-rCD2* (**d**). Candidate cell-surface molecules are overexpressed only in Mz19 PNs. **b-c**, Or47b axons and Mz19 dendrites do not overlap in control (**b**), but form ectopic connections following Ten-m overexpression (**c**), as seen by axon-dendrite intermingling (arrowhead). **e-f**, Or88a axons and Mz19 dendrites connect at the VA1d glomerulus in control (**e**), but the connection is partially lost following Ten-a overexpression, as part of Or88a axons no longer intermingle with Mz19 dendrites (arrowhead). Target areas of Or47b (**b-c**) or Or88a (**e-f**) axons are outlined. Mismatching phenotypes are quantified in Fig. S9k and S10q. The first three columns in **b,c,e,f** show separate channels of the same section; the fourth shows higher magnification of the dashed squares (as in Fig. 3, 4, 5d-g.). Unless indicated, all images in this and subsequent figures are single confocal sections and all scale bars are 10 μm . **g**, Domain composition of *Drosophila* Ten-m and Ten-a. **h**, Phylogeny of the *Drosophila* Teneurins and related proteins in other species. Branch lengths represent units of substitutions per site of the sequence alignment. Teneurins are evolutionarily conserved in bilaterians and a unicellular choanoflagellate *Monosiga brevicollis*, but not in cnidarians.

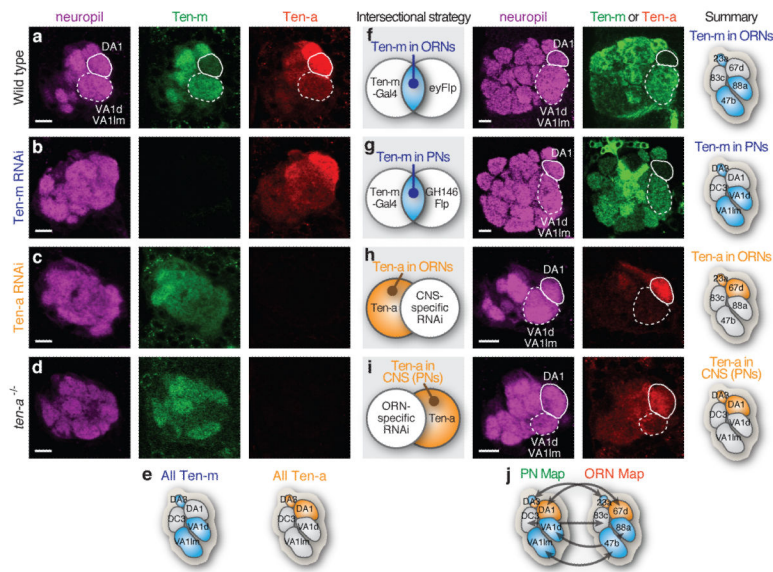


Figure 2. Teneurins are differentially expressed in matching PN and ORN classes

a. Developing antennal lobes at 48 hrs APF stained by antibodies against Ten-m, Ten-a, and a neuropil marker, N-cadherin. Solid lines encircle the DA1 glomerulus (Ten-m low, Ten-a high). Dashed lines encircle the VA1d/VA1lm glomeruli (Ten-m high, Ten-a low). **b-c.** Ten-m and Ten-a proteins are undetectable following pan-neuronal RNAi of *ten-m* (**b**) and *ten-a* (**c**), respectively. **d.** A *ten-a* homozygous mutant eliminated the Ten-a antibody staining. **e.** Summary of elevated Ten-m and Ten-a expression in five select glomeruli. **f-g.** Expression of the Flp-out GFP reporter *UAS>stop>mCD8GFP* at the intersection of *ten-m-GAL4* with ORN-specific *ey-Flp* (**f**) or with PN-specific *GH146-Flp* (**g**) in adult. **h-i.** Antibody staining of Ten-a in central neuron-specific RNAi (**h**) or in ORN-specific RNAi (**i**) at 48 hrs APF. Individual cell type-specific Teneurin expression patterns are schematically summarized at right (**f-i**). **j.** Combined expression patterns of Teneurins in PNs (left) and ORNs (right). Blue: Ten-m high; orange: Ten-a high.

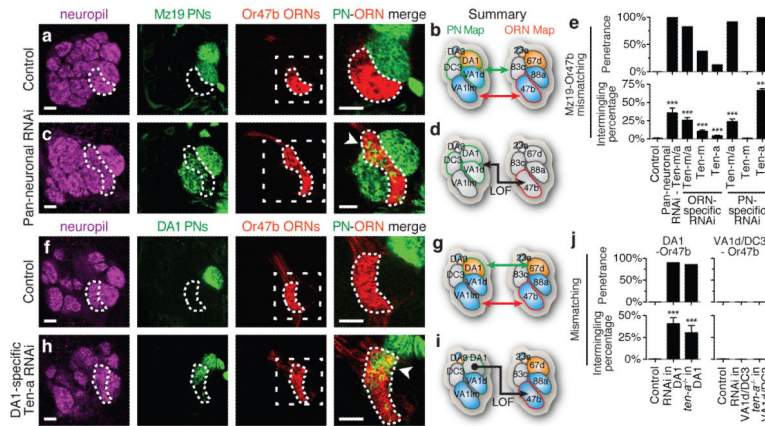


Figure 3. Loss of Teneurins causes PN-ORN mismatching

a, Normally, Mz19 dendrites (green) innervate glomeruli adjacent to the VA1Im glomerulus, which is itself innervated by Or47b axons (red). The dashed line encircles Or47b axons. DC3 PNs are located posterior to DA1/VA1d PNs and Or47b ORNs, and are not visible in these sections. **c**, Mismatching phenotypes in *ten-m* and *ten-a* RNAi driven by the pan-neuronal driver *C155-GAL4*. Dashed lines encircle Or47b ORN axons, showing intermingling with Mz19 PN dendrites (arrowhead). **e**, Quantification of Mz19-Or47b mismatching phenotypes. For all genotypes, *n* = 15. **f**, In control, DA1 PNs do not intermingle with Or47b ORNs. **h**, MARCM expression of *ten-a* RNAi in DA1 PNs causes dendrite intermingling with Or47b axons (arrowhead). **j**, Quantification of mismatching phenotypes. For all genotypes, *n* = 6. Error bars represent S.E.M. ***, *p* < 0.001 compared to control. **b, d, g, i**, Summary showing normal connectivity in control (**a, f**) and mismatching phenotypes following *teneurin* RNAi (**c, h**). Blue: Ten-*m* high; orange: Ten-*a* high. Green outlines: labeled PNs. Red outlines: labeled ORNs.

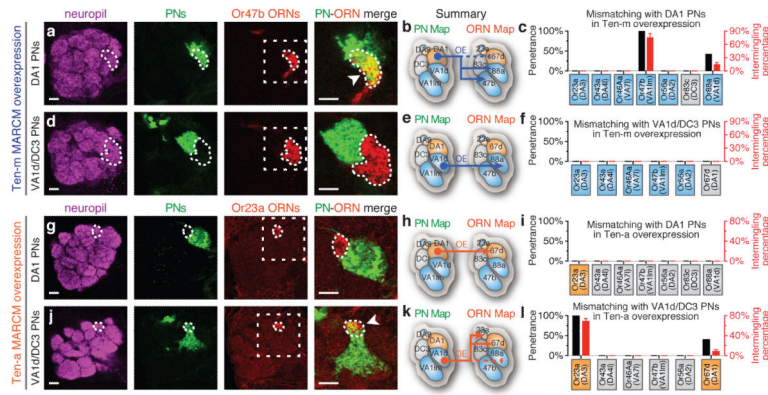


Figure 4. Teneurin overexpression in specific PN classes causes mismatching
 Mismatching phenotypes following Ten-m (a-f) or Ten-a (g-l) overexpression in different PN classes. Specific PN classes are labeled by MARCM with *Mz19-GAL4* and ORN axons using *Or47b-rCD2* (a, d) or *Or23a-mCD8GFP* (g, j). In control, *Mz19* PNs do not intermingle with *Or47b* ORNs (Fig. 1b). MARCM overexpression of Ten-m in DA1 PNs (a, arrowhead), but not VA1d/DC3 PNs (d), causes dendrite mismatching with *Or47b* axons. MARCM overexpression of Ten-a in VA1d/DC3 PNs (j, arrowhead), but not in DA1 PNs (g), causes their dendrites to mismatch with *Or23a* axons. (c, f, i, l) Quantification of mismatching phenotypes (n=9 for each). Error bars represent S.E.M. See Fig. S10 for details on some genotypes quantified here. (b, e, h, k) Schematic summarizing the mismatching phenotypes in Fig. 4, Fig. S9, and Fig. S10. Blue: Ten-m high; orange: Ten-a high.

